LCTS/2014-23

The Dark Side of θ_{13}, δ_{CP}, Leptogenesis and Inflation in Type-I Seesaw

Wei-Chih Huang[a,1]

[a] *Department of Physics and Astronomy, University College London, UK*

arXiv:1405.5886v3 [hep-ph] 17 Nov 2014

Abstract

In the context of the type-I seesaw mechanism, it is known that θ_{13} is zero and leptogenesis can not be realized if there exists a residual flavor symmetry resulting in the Tri-Bimaximal neutrino mixing pattern. We propose a simple framework where additional particles, odd under a Z_2 symmetry, break the residual flavor symmetry and the lightest of the Z_2 odd particles is the dark matter candidate. As as result, nonzero θ_{13}, δ_{CP}, leptogenesis and the correct dark matter density can be accommodated. On the other hand, a Z_2 odd scalar can play the role of the inflaton with mass of 10^{13} GeV motivated by the recent BICEP2 results. Interestingly, the model can "generate" $\delta_{CP} \simeq -\pi/2$, preferred by the T2K experiment in the normal hierarchy neutrino mass spectrum.

[1] *wei-chih.huang@ucl.ac.uk*

1 Introduction

Although the evidence for massive neutrinos and the existence of Dark Matter (DM) is well established, neither of them can be explained by the Standard Model (SM). The simplest extension to the SM for providing a mass to neutrinos is to introduce extra SM gauge singlet fermions, coupling to the active neutrinos and the Higgs boson via Yukawa couplings, the so-called type-I seesaw [1]. At the same time, any additional SM gauge singlet, with a symmetry to guarantee its stability or having a long lifetime compared to the age of the universe, can be the DM candidate. The main idea of this work is to make a connection between DM and the neutrino sector based on the following observations.

The active neutrino mixing matrix, the Pontecorvo-Maki-Nakagawa-Sakata matrix U_{PMNS}, can be well approximated by the Tri-Bimaximal Mixing (TBM) pattern [2–7] if the third neutrino mixing angle θ_{13} is zero. There have been many models based on discrete flavor symmetries that can naturally create the TBM pattern. Some of them are A_4, for example, Refs. [8–14], S_4 [15–19], and T' [20–22], etc. The idea behind these models is to look for proper group representations for particles in question such that after scalars in the model obtain Vacuum Expectation Values (VEVs) which break the flavor symmetry, the neutrino mixing matrix features the TBM pattern resulting from the residual flavor symmetry. The discovery of non-vanishing θ_{13} in reactor neutrino experiments [23–25] (also [26,27]), however, demands breaking of the discrete symmetry.

On the other hand, it has been shown in Ref. [28] (also Refs. [29–32]) that in the type-I seesaw with non-degenerate neutrino spectra, the R matrix in the Casas-Ibarra parametrization [33] is simply a diagonal matrix with elements being ± 1, if there is an underlying discrete flavor symmetry at work. As a consequence, the lepton asymmetry, which is proportional to the imaginary part of R, vanishes. The underlying reason is that the discrete flavor symmetry usually leads to the form-diagonalizable [34] neutrino mass matrix, i.e., neutrino masses are completely independent of the mixing matrix elements. In other words, input parameters determining the masses are not related to those determining the mixing angles and phases. The form-diagonalizable property reduces the number of parameters in the rotation matrices used to diagonalize the full neutrino matrix (including both heavy and light neutrinos), leaving R the unit matrix up to a minus sign. Alternatively, another explanation is based on the idea of Form Dominance (FD), that is the requirement that each column of the Dirac mass matrix in the flavor basis is proportional to a different column of the PMNS matrix [14,35]. The type-I seesaw with a flavor symmetry has the FD property.

In this paper, we propose a simple framework, where the underlying flavor symmetry is broken by additional "dark" particles, odd under an imposed Z_2 symmetry: an $SU(2)_L$ singlet fermion χ_1, which is the DM candidate, and a fermonic $SU(2)_L$ doublet χ_2 and a real gauge-singlet scalar S. The radiative corrections from these particles to the Dirac mass matrix violate the flavor symmetry, leading to nonzero θ_{13} and leptogenesis. The connection between the CP-violation phase δ_{CP} in U_{PMNS} and leptogenesis will be established if the only source of CP-violation comes from the radiative corrections. We also explore the possibility of S

being the inflaton motivated by the recent BICEP2 results on the scalar-to-tensor ratio [36]. All in all, we explore the interplay among θ_{13}, δ_{CP}, leptogenesis, DM and inflation. Instead of presenting a concrete flavored DM model, we search for a minimum setup with the smallest set of parameters to achieve non-vanishing θ_{13} and leptogenesis, assuming the flavor symmetry yields the TBM pattern. For discussions on flavored DM models, see Refs. [37–45] and the recent review [46]. Note that the idea of connecting DM to flavor symmetry breaking (and hence θ_{13} or leptogenesis) has been proposed before, for example, in Refs. [35, 47–51]. This work has two distinctive features. The first is the radiative correction arises in the Dirac mass matrix, instead of the light neutrino mass matrix. Second, our dark matter candidate is *not* one of right-handed neutrinos, which are even under the Z_2 symmetry in this model.

This paper is organized as follows. In Section 2, we specify the particle content and quantum numbers. Section 3 is devoted to the study of the radiative corrections to θ_{13} from the dark particles. We discuss the DM relic density in section 4 via annihilations through Higgs exchange, and leptogenesis in Section 5 by including new contributions from χ's and S. We present the results in Section 6, considering the DM density, θ_{13} and leptogenesis. S being the inflaton is discussed in Section 7. We conclude in Section 8.

2 Model and Observables

The model consists of three heavy right-handed neutrinos, N_1, N_2 and N_3 with $m_{N_3} \geq m_{N_2} \geq m_{N_1}$. In addition, we have a gauge-singlet fermion χ_1, an fermionic $SU(2)_L$ doublet χ_2, and a real gauge-singlet scalar S. Moreover, we impose a Z_2 symmetry under which χ_1, χ_2 and S are odd, to guarantee the stability of the DM candidate, χ_1. The Lagrangian reads[1]

$$\mathcal{L} \supset y_{\alpha i}\ (L_\alpha \cdot H)\, N_i - \frac{M_i}{2} N_i N_i + \lambda_\alpha\ (L_\alpha \cdot \chi_2)\, S + \lambda_{H\chi}\ \left(\chi_2 \cdot \tilde{H}\right) \chi_1 + \lambda_{N_i}\, \chi_1 N_i S + h.c.\,, \quad (2.1)$$

where $L_\alpha = (\nu_\alpha\ e_\alpha)^T$ and $\alpha = (e, \mu, \tau)$. H is the SM Higgs doublet, and "$\cdot$" refers to $SU(2)$ multiplication to form a singlet. An additional $SU(2)_L$ doublet $\tilde{\chi}_2$, with an opposite $U(1)_y$ charge to χ_2, is also introduced to make the model anomaly-free. We omit mass terms for $\chi_{1,2}$ and S, which are not relevant here, and will explicitly specify them when discussing the DM phenomenology. The quantum numbers of the model are shown in Table 1. Notice that the Lagrangian is invariant under the $SU(2)_L \times U(1)_y$ gauge symmetry but does not necessarily preserve the underlying residual flavor symmetry responsible for the TBM pattern. In fact, we *do* require residual flavor symmetry breaking to have $\theta_{13} \sim 9^\circ$. We provide a simple model based on the A_4 symmetry in Appendex A to realize the Lagrangian, Eq. 2.1. The goal of this work, however, is to look for the minimum setup to achieve non-vanish θ_{13} without looking into details of the flavor charge assignment.

In this work, we consider the observed U_{PMNS} mixing angles and the light neutrino mass-squared differences, the DM relic density and the baryon density, presented in Table 2. In

[1]The two-component spinor notation has been used throughout the paper, unless noted otherwise.

Field	L	H	N_1	N_2	N_3	χ_1	χ_2	$\tilde{\chi}_2$	S
$SU(2)_L$	2	2	1	1	1	1	2	2	1
$U(1)_Y$	-1/2	1/2	0	0	0	0	1/2	-1/2	0
Z_2	+	+	+	+	+	−	−	−	−

Table 1: *The particle content and corresponding quantum numbers in the model.*

Section 3, we fit to only the U_{PMNS} angles and the mass-squared differences in order to show how the existence of χ's and S can modify U_{TBM} in both the Normal Hierarchy (NH) and Inverted Hierarchy (IH) neutrino mass spectra, while in Section 6 we fit to all observables listed in Table 2.

	$\sin^2 2\theta_{12}$	$\sin^2 2\theta_{23}$	$\sin^2 2\theta_{13}$	Δm^2_{sol} (eV^2)	$\lvert\Delta m^2_{atm}\rvert$ (eV^2)	$\Omega_{\rm b}h^2$	$\Omega_{\rm DM}h^2$
best-fit	0.857	1	0.095	7.50×10^{-5}	2.32×10^{-3}	0.022	0.120
1σ	0.024	0.301	0.01	2×10^{-6}	1×10^{-4}	3.3×10^{-4}	3.1×10^{-3}

Table 2: *The best-fit value and* 1σ *standard deviation of relevant observables included in this paper. The values are taken from Refs. [52–54].*

3 Nonzero θ_{13}

The idea of this paper is to explore a scenario where the particles odd under the Z_2 symmetry break the underlying flavor symmetry[2] and we choose the flavor symmetry to reproduce the TBM pattern[3] featuring zero θ_{13}:

$$U_{TBM} = \begin{pmatrix} \sqrt{\frac{2}{3}} & \frac{1}{\sqrt{3}} & 0 \\ -\frac{1}{\sqrt{6}} & \frac{1}{\sqrt{3}} & \frac{1}{\sqrt{2}} \\ -\frac{1}{\sqrt{6}} & \frac{1}{\sqrt{3}} & -\frac{1}{\sqrt{2}} \end{pmatrix}. \tag{3.1}$$

Then we investigate how the existence of DM can perturb U_{TBM} into U_{PMNS} with $\theta_{13} \sim 9^\circ$. The 6-by-6 neutrino mass matrix is

$$m = \begin{pmatrix} 0 & m_D \\ m_D^T & M \end{pmatrix}, \tag{3.2}$$

where m_D is the Dirac mass matrix and M is the heavy neutrino mass matrix. As shown in Ref. [28], if there is an underlying flavor symmetry at work, m_D can be completely determined

[2]As we mentioned above, the underlying flavor symmetry has been broken by VEVs of scalars charged under the flavor symmetry. The residual symmetry leads to the TBM pattern. From now on, flavor symmetry refers to "residual" flavor symmetry, unless noted otherwise.

[3]In general, one can repeat the procedure for arbitrary mixing patterns.

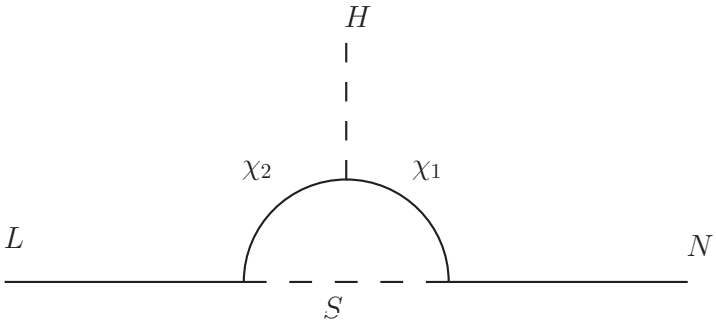

Figure 1: *DM corrections to the Dirac neutrino mass, m_D.*

by the light and heavy neutrino masses, $m_{\nu_{1,2,3}}$ and $m_{N_{1,2,3}}$, up to phases, in a basis where M $(= \text{diag}(m_{N_a}, m_{N_b}, m_{N_c}))$ is diagonal, i.e.,

$$m_D^0 = U_{TBM} P \begin{pmatrix} \sqrt{m_{\nu_1}} & 0 & \\ 0 & \sqrt{m_{\nu_2}} & 0 \\ 0 & 0 & \sqrt{m_{\nu_3}} \end{pmatrix} \begin{pmatrix} \sqrt{m_{N_a}} & 0 & \\ 0 & \sqrt{m_{N_b}} & 0 \\ 0 & 0 & \sqrt{m_{N_c}} \end{pmatrix}. \tag{3.3}$$

Here, $P = \text{diag}(e^{i\gamma_1}, e^{i\gamma_2}, e^{i\gamma_3})$ can, in principle, be absorbed into Majorana phases and is not relevant for this work. Note that we do *not* assume $m_{N_a} \leq m_{N_b} \leq m_{N_c}$ and that is why we use $N_{a,b,c}$ instead of $N_{1,2,3}$. The superscript 0 on m_D refers to the unperturbed m_D coming from U_{TBM} only.

As shown in Fig. 1, the dark particles running in the loop (DM Loop hereafter) can contribute to m_D, which in turn changes the neutrino mixing matrix, and the radiative corrections can be written as,

$$\delta m_D = \frac{\langle H^0 \rangle}{\sqrt{2}} \lambda_{H\chi} \begin{pmatrix} \lambda_e \lambda_{N_a} & \lambda_e \lambda_{N_b} & \lambda_e \lambda_{N_c} \\ \lambda_\mu \lambda_{N_a} & \lambda_\mu \lambda_{N_b} & \lambda_\mu \lambda_{N_c} \\ \lambda_\tau \lambda_{N_a} & \lambda_\tau \lambda_{N_b} & \lambda_\tau \lambda_{N_c} \end{pmatrix} f_{loop}, \tag{3.4}$$

where f_{loop} is the loop function and $\langle H^0 \rangle = v$ (~ 246) GeV is the Higgs VEV.

In this paper, instead of performing detailed parameter space scans as done in Refs. [55–57], we keep a spirit of minimality in mind, managing to find a minimal model with the fewest parameters to realize dynamical breaking of the flavor symmetry through the DM loop. Thus, we use the benchmark point in Table 3 with $(N_a, N_b, N_c) = (N_1, N_2, N_3)$. In fact, as long as the heavy neutrino masses are of the same order, $\theta_{13} \sim 9^\circ$ can always be obtained regardless of the ordering of m_{N_a}, m_{N_b} and m_{N_c}. The mass-squared differences, $m_{\nu_2}^2 - m_{\nu_1}^2$ and $|m_{\nu_3}^2 - m_{\nu_2}^2|$, are fixed to the observed values Δm_{sol}^2 and Δm_{atm}^2 from solar and atmospheric neutrino oscillation experiments.[4] With zero $\lambda_{N_{a(=1)}}$, $\lambda_{N_{b(=2)}}$ and λ_τ, the DM loop radiative corrections

[4]Note that $m_{\nu_{1,2,3}}$ as input parameters, may *not* be the same as the resulting light neutrino masses once the DM loop contributions are taken into account. In other words, by fixing the unperturbed Δm^2 to be the observed ones, it implies the DM loop can not modify Δm^2 significantly.

contribute to the $(1,3)$ and $(2,3)$ elements of the Dirac mass matrix m_D, denoted as $(\delta m_D)_{13}$ and $(\delta m_D)_{23}$, respectively.

We should mention that the sum of light neutrino masses, $\sum_i m_{\nu_i}$, is roughly bounded below 0.3 eV from cosmological constraints from Refs. [54, 58–63]. In fact, $m_{\nu_3} = 0.1$ eV is in tension with some of the references.

	m_{ν_1} (eV)	m_{ν_2} (eV)	m_{ν_3} (eV)	λ_{N_a}	λ_{N_b}	λ_τ
NH	0	8.66×10^{-3}	4.89×10^{-2}	0	0	0
IH	1.107×10^{-1}	1.11×10^{-1}	0.1	0	0	0
	m_{N_1} (GeV)	m_{N_2} (GeV)	m_{N_3} (GeV)	m_S (GeV)	m_{χ_1} (GeV)	m_{χ_2} (GeV)
NH/IH	1000	$1000 + \Delta m_{N_{12}}$	2000	700	62	200

Table 3: *The benchmark point for the NH and IH cases. We here keep $m^2_{\nu_2} - m^2_{\nu_1}$ and $|m^2_{\nu_3} - m^2_{\nu_2}|$ to be Δm^2_{sol} and Δm^2_{atm}, respectively. The reason why $m_{\chi_1} \sim m_h/2$ comes from the resonant enhancement from the DM consideration as we shall see below. In addition, we also need $\Delta m_{N_{12}} \equiv m_{N_2} - m_{N_1} \sim \Gamma_{N_2}$ (decay width of N_2) for the resonant enhancement to realize low-scale leptogenesis.*

For the fitting procedure, we first compute the modified light neutrino mass spectrum and the mixing angles as the functions of λ_e and λ_μ with the benchmark point in Table 3 and $\lambda_{N_c} = 1$. Then, we fit to the observed U_{PMNS} angles and the mass-squared differences shown in Table 2. The results are shown in Fig. 2, with 68% (dark blue) and 99% (light blue) confidence region. Note that given the neutrino mass matrix m, there are ambiguities on determining the mixing angles of U_{PMNS}. To be more concrete, any equivalent transformation, $U'_{PMNS} \to P_1 U_{PMNS} P_2$ in which $P_{1,2}$ are diagonal matrices with elements of ± 1, renders intact the physical observables, such as oscillation probabilities, but will correspond to different active mixing angles. As demonstrated in Refs. [64, 65], all mixing angles can be chosen positive and smaller than or equal to $\pi/2$ provided δ_{CP} is allowed to vary between $-\pi$ and π. For this reason, we choose to use $\sin^2 2\theta$'s in the fit, which are free from ambiguities.

Remarkably, λ_e (and λ_{N_c}) alone can amend m_D to produce desired U_{PMNS} and Δm^2, for both IH and NH.[5] In the NH situation, this can be understood by simply looking at the perturbed m_D (with m_{ν_1}=0) including λ_e and λ_{N_c} only,

$$m_D = m_D^0 + \delta m_D = \begin{pmatrix} 0 & \sqrt{\frac{m_{N_b} m_{\nu_2}}{3}} & (\delta m_D)_{13} \\ 0 & \sqrt{\frac{m_{N_b} m_{\nu_2}}{3}} & -\sqrt{\frac{m_{N_c} m_{\nu_3}}{2}} \\ 0 & \sqrt{\frac{m_{N_b} m_{\nu_2}}{3}} & \sqrt{\frac{m_{N_c} m_{\nu_3}}{2}} \end{pmatrix}, \tag{3.5}$$

[5]For the IH case, the reason why m_{ν_3} has to be nonzero is we constrain ourselves to real λ_e and λ_μ. With complex λ's, zero m_{ν_3} can be achieved.

and the light neutrino mass matrix is

$$
\begin{aligned}
m_\nu &\sim -m_D M^{-1} m_D^T \qquad (3.6)\\
&= -\begin{pmatrix}
\frac{(\delta m_D)_{13}^2}{m_{N_c}} + \frac{m_{\nu_2}}{3} & -(\delta m_D)_{13}\sqrt{\frac{m_{\nu_3}}{2m_{N_c}}} + \frac{m_{\nu_2}}{3} & (\delta m_D)_{13}\sqrt{\frac{m_{\nu_3}}{2m_{N_c}}} + \frac{m_{\nu_2}}{3} \\
-(\delta m_D)_{13}\sqrt{\frac{m_{\nu_3}}{2m_{N_c}}} + \frac{m_{\nu_2}}{3} & \frac{m_{\nu_2}}{3} + \frac{m_{\nu_3}}{2} & \frac{m_{\nu_2}}{3} - \frac{m_{\nu_3}}{2} \\
(\delta m_D)_{13}\sqrt{\frac{m_{\nu_3}}{2m_{N_c}}} + \frac{m_{\nu_2}}{3} & \frac{m_{\nu_2}}{3} - \frac{m_{\nu_3}}{2} & \frac{m_{\nu_2}}{3} + \frac{m_{\nu_3}}{2}
\end{pmatrix},
\end{aligned}
$$

where $(\delta m_D)_{13}$ denotes the DM loop contribution. The existence of $(\delta m_D)_{13}$ explicitly breaks the residual $\mu - \tau$ symmetry, making $\theta_{13} \neq 0$ [66]. In addition, we have $(\delta m_D)_{13} \sim 10^{-7}$ GeV from the confidence region in Fig. 2, and in turn $\frac{(\delta m_D)_{13}^2}{m_{N_c}} \ll \frac{m_{\nu_2}}{3}$ so that the trace of m_ν, the sum of three light neutrino masses, remains unchanged, i.e., the mass-squared differences stay intact. The reason why $(\delta m_D)_{13}$ is so small is that the neutrino mass-squared differences are fixed to the experimental values in the benchmark points so that the radiative correction is forced to be small in order to reproduce the neutrino oscillation observables. In summary, the DM loop with λ_e (and λ_{N_c}) induces the $\nu_e - N_c$ mixing which then breaks the $\mu - \tau$ symmetry to generate sizable θ_{13} but keep the light neutrino mass spectrum unscathed. We refer readers to Ref. [67], where different breaking patterns on the $\mu - \tau$ symmetry have been studied systematically, and also Refs. [4, 68] on modifications or radiative corrections to the TBM pattern. Furthermore, $(\delta m_D)_{13}$ is the only radiative correction that can change U_{TBM} into U_{PMNS} and have the correct mass-squared differences on its own. One must need at least two radiative corrections to achieve the goals if $(\delta m_D)_{13}$ is not involved[6].

It is worthwhile to mention that the DM loop, in addition to a real component, would have an imaginary part if the internal particles are on-shell. One might naively conclude it could contribute to a CP-violating phase in U_{PMNS}. It, however, is a false statement since first the corresponding antiparticles would have the identical loop structure with the same imaginary part due to CPT invariance, i.e., the imaginary part gives rise to a CP-conserving phase. Second, this type of the CP-conserving phase should not be taken into account when diagonalizing the neutrino mass matrix but should be absorbed into the decay width of the heavy neutrinos. On the other hand, the CP-conserving phase does play a role in the context of leptogenesis as discussed below.

We conclude this section with Fig. 3, where the DM loop involves λ_e only. m_{ν_1} (m_{ν_3}) for NH (IH) and λ_e are being varied to find the minimum χ^2, while the same set of mass parameters as above are assumed. It is clear that in the NH case, small m_{ν_1} is preferred and λ_e is nearly constant in the confidence region because of negligible contributions from nearly zero m_{ν_1}. On the other hand, for the IH case, large m_{ν_3} ($\gtrsim 0.1$ eV) is preferred, which is compensated by small λ_e. The different behaviors can be simply understood by looking into the Dirac mass matrix, m_D. In the NH case, δm_D from the DM loop and terms involving m_{ν_1} are located in the third and first column, respectively, while for IH, they both appear in the third column. As a consequence, when solving for the light neutrino masses and U_{PMNS}, the magnitude of m_{ν_3} is correlated with λ_e in IH whereas λ_e is nearly independent of m_{ν_1} in NH.

[6]This conclusion might change if input parameters, Δm_{12}^2 and Δm_{23}^2, are allowed to vary.

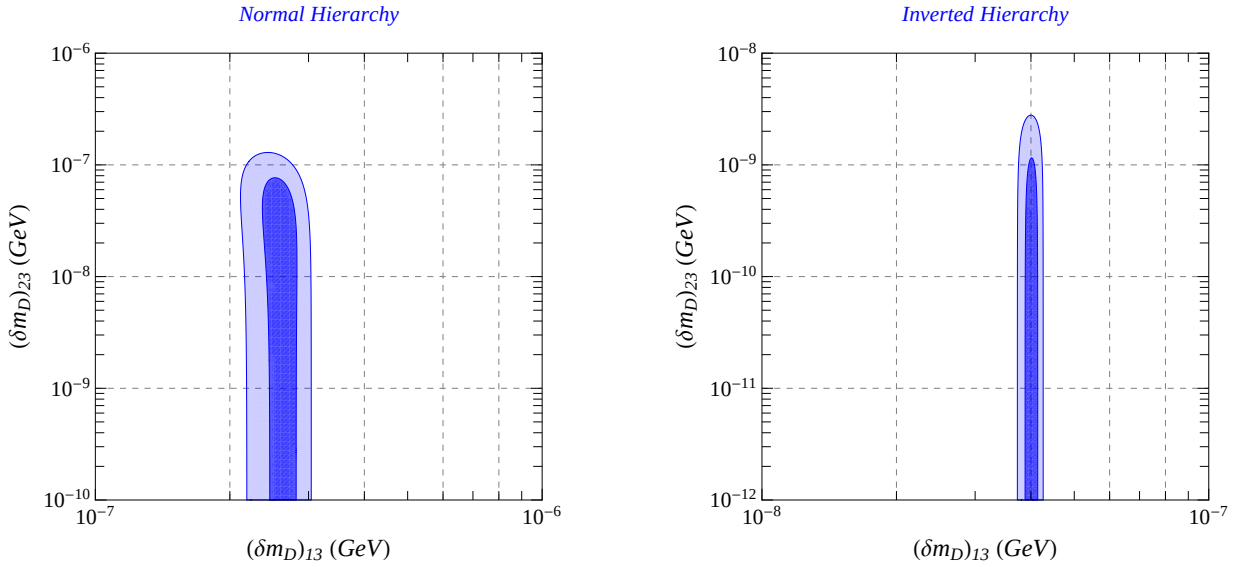

Figure 2: *Confidence region on* $(\delta m_D)_{13}$ *and* $(\delta m_D)_{23}$ *to reproduce the observed neutrino mixing angles and the mass-squared differences via the DM loops using the benchmark point in Table 3 with* $(N_a, N_b, N_c) = (N_1, N_2, N_3)$*. For the NH case, the best reduced* χ^2*,* χ^2 *per degree of freedom, is 0.46 while the reduced* χ^2 *is 1.29 for IH.*

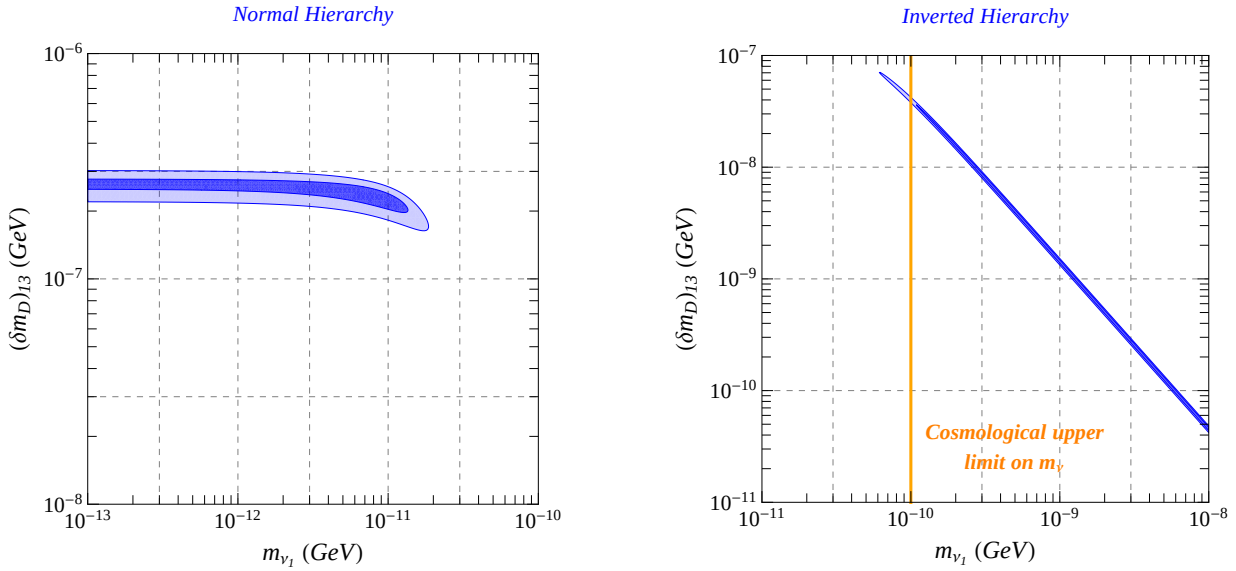

Figure 3: *Confidence region on* $m_{\nu_{1,3}}$ *and* $(\delta m_D)_{13}$ *to reproduce the observed neutrino mixing angles and the mass-squared differences via the DM loops using the benchmark point shown in Table 3 with* $(N_a, N_b, N_c) = (N_1, N_2, N_3)$*. Note that only a single DM radiative correction,* $(\delta m_D)_{13}$*, is included in the fit. For the NH case, the best reduced* χ^2 *is 0.25, while the reduced* χ^2 *is 0.37 for IH. We also show the cosmological constraint [54, 58–63] on the neutrino mass.*

4 DM Relic Density

In this Section, we compute the DM relic abundance through χ_1 annihilations. We begin with the relevant Lagrangian for the DM relic density,

$$\begin{aligned}\mathcal{L} \supset \quad & \lambda_{H\chi}\left(\chi_2 \cdot \tilde{H}\right)\chi_1 + \lambda_{H\tilde{\chi}}\left(\tilde{\chi}_2 \cdot H\right)\chi_1 + \lambda_\alpha\left(L_\alpha \cdot \chi_2\right)S \\ & + \lambda_{N_i}\,\chi_1 N_i S - \frac{1}{2}m_S^2 - \frac{1}{2}m_{\chi_1}\chi_1\chi_1 - m_{\chi_2}\tilde{\chi}_2\chi_2 + h.c.,\end{aligned} \tag{4.1}$$

where $H = \frac{1}{\sqrt{2}}(0\,,\, v+h)^T$, in which h is the Higgs boson field. After electroweak symmetry breaking, χ_1 generally mixes with the neutral components of χ_2 and $\tilde{\chi_2}$, referred as χ_2^0 and $\tilde{\chi}_2^0$, respectively; therefore DM is the linear combination of χ_1, $\tilde{\chi}_2^0$ and χ_2^0. The DM relic abundance is determined by the processes shown in Fig. 4, where m denotes the mass eigenstate. The first process is, however, kinematically suppressed since $m_N \gtrsim m_{\chi_1} + m_{\chi_2}$ due to the leptogenesis consideration as we shall see below. For the Higgs exchange process, for simplicity, we assume $m_{\chi_2} > m_{\chi_1}$ so that co-annihilation processes are negligible.

In this framework, Direct Detection (DD) constraints, especially those set by LUX [69] on Spin-Independent (SI) interactions, should be considered since χ_1^m can also interact with nucleons via t-channel Higg-mediated processes. We show the annihilation cross-section and the SI DM-nucleon cross-section in Appendix B. It turns out the required $\lambda_{H\chi}$'s in order to produce the correct DM density will also generate a large DM-nucleon cross-section, in conflict with the LUX results. There are at least two solutions – resonant enhancement and co-annihilation.

1. One can make $m_{\chi_1} \sim m_h/2$ to enhance the annihilation cross-section by virtue of the small Higgs decay width (~ 4 MeV [70]) to keep $\lambda_{H\chi}$ small enough not to be excluded by the LUX DD bounds. From Fig. 5, we show the LUX constraints on $\lambda_{H\chi}$ and the $\chi_1 - \chi_2$ mixing, θ. It is clear that only when $m_{\chi_1} \sim m_h/2$, can χ_1 annihilation be sufficient enough to have the correct density without inducing the large SI DM-nucleon cross-section, avoiding the LUX bounds. As a consequence, we pick $m_{\chi_1} = 62$ GeV as our benchmark point.[7]

2. The second method is to make $m_{\chi_2} \gtrsim m_{\chi_1}$ to turn on co-annihilation processes such that the DM density is mostly determined by co-annihilation which is not constrained by DD, as long as the mass-splitting is much larger than the typical nuclear recoil energy of order $\mathcal{O}$(KeV) in DD experiments. This solution is quite fine-tuned since, in this setup, annihilation and co-annihilation cross-section are generally of the same order.

In principle, one should also take into account processes mediated by the Z boson. For DM annihilation, we simply chose $\lambda_{H\chi} \sim \lambda_{H\tilde{\chi}}$ and $m_{\chi_2} \sim m_{\tilde{\chi}_2}$ so that after diagonalizing the mass

[7]For the resonant region, χ_1 mostly annihilates into b-quarks, which in turn produce protons and antiprotons in addition to gamma rays. Stringent limits on the b-quark final state is recently derived in Ref. [71], based on indirect DM searches. We would like to point out these limits become much weaker in our model since the annihilation cross-section is velocity suppressed and the current DM velocity is very small ($\sim 10^{-3}$).

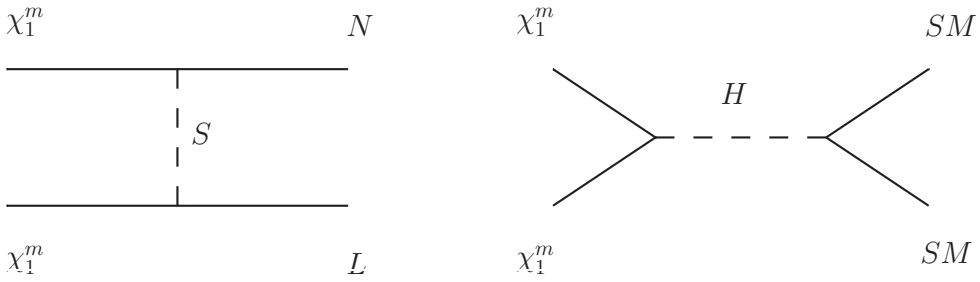

Figure 4: *Annihilation processes of χ_1^m, where m refers to the mass eigenstate.*

matrix of χ's, the DM particle has roughly equal χ_2 and $\tilde{\chi}_2$ component, and consequently does not strongly interact with Z since χ_2 and $\tilde{\chi}_2$ carry opposite charges. As a result, the Higgs exchange processes mentioned above will be the dominant contribution. In terms of DD experiments, because of the negligible mixing between χ_1 and χ_2's, the DM particle is mostly χ_1, that is a Majorana particle. It has only Spin-Dependent (SD) interactions with nucleons through vector boson exchange. The DD bounds on SD interactions are much weaker and thus will not be considered here.

5 Leptogenesis with TeV N_1

In this section, we study the lepton asymmetry generated from N_1 decays, including additional contributions from the dark particles χ's and S. The heavy neutrino mass in question is of order TeV, as shown in Table 3. Fig. 6 shows the relevant Feynman diagrams for leptogenesis and here we only show $N \to H^+ L^-$ for demonstration.[8]

If there are no DM loop contributions, because of the flavor symmetry the R matrix is real, leading to zero lepton asymmetry from N_1 decays. Additionally, even if R is complex, the generated lepton asymmetry is still too small to account for the observed baryon asymmetry as shown in Ref. [73]: m_{N_1} has to be larger than 10^9 GeV in order for leptogenesis to work in the type-I seesaw.

On the other hand, the DM loop can interfere with the tree-level diagram ($N \to HL$) to induce the lepton asymmetry. Besides, the R matrix, which was real in the presence of the exact flavor symmetry, can become complex due to phases in the DM loop and the lepton asymmetry can be generated via conventional leptogenesis as shown in the top panels of Fig. 6. Nonetheless, it is usually suppressed compared to the one coming from the direct interference between $N \to HL$ and the DM loops, the lower panels of Fig. 6, because of loop suppression and smallness of Yukawa couplings, $y_{\alpha i} \sim 10^{-6}$ for $m_{N_i} \sim$ TeV.

[8] The arrow on fermion lines represents the chirality of particles and we use the convention in Ref. [72], i.e., a particle with the arrow pointing in the same direction as the four momentum is left-handed. We refer readers to the reference for the details of two-component Weyl-spinor notations and computation techniques. Here, we show only the vertex contribution (top right panel) as a representative of type-I seesaw loop diagrams. In fact, the wave function contribution is also included in computation.

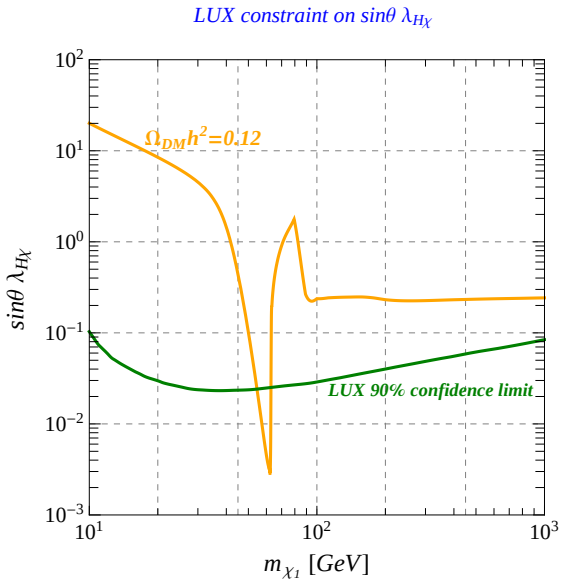

Figure 5: *LUX bounds on the product of* $\sin\theta$ *and* λ_H*, where* θ *is the* $\chi_1 - \chi_2$ *mixing angle. The Orange line corresponds to the correct DM density, where only annihilation via Higgs exchange is taken into account. The green line is the LUX* 90% *confidence limit on SI interactions [69]. It is clear only the resonant region is not excluded by the LUX results; therefore we choose* $m_{\chi_1} = 62$ *GeV as our benchmark point.*

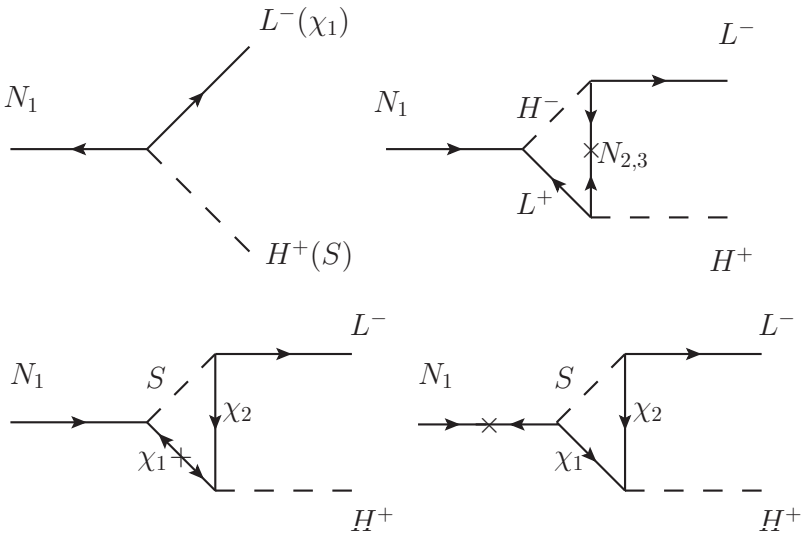

Figure 6: *Processes relevant for leptogenesis including additional contributions from* χ*'s and* S*.*

Before computing the lepton asymmetry, one has to remember that in order to obtain nonzero results from tree- and loop-level interference, two conditions must be satisfied – internal particles in the loop should be on-shell and the product of couplings of the tree- and loop-diagram must have a nonzero imaginary part. Failing to satisfy either results in zero lepton asymmetry. As long as N_1 is heavier than the sum of χ_1 and S mass, which is the case in this work, the first condition holds. To elaborate the second one, we have to look at the relevant terms involved in the loop:

$$\mathcal{L} \supset \lambda_\alpha \left(L_\alpha \cdot \chi_2\right) S + \lambda_{H\chi} \left(\chi_2 \cdot \tilde{H}\right) \chi_1 + \lambda_{N_1}\, \chi_1 N_1 S. \tag{5.1}$$

Assuming all couplings are complex to begin with: $\lambda_\alpha = |\lambda_\alpha| e^{i\theta_\alpha}$, $\lambda_{H\chi} = |\lambda_{H\chi}| e^{i\theta_H}$ and $\lambda_{N_1} = |\lambda_{N_1}| e^{i\theta_1}$, we can make $\lambda_{H\chi}$ real by redefining $\chi_2 \to \chi_2 e^{i\theta_H}$. Consequently, we can redefine $\tilde{\chi}_2 \to \tilde{\chi}_2 e^{-i\theta_H}$, such that $e^{i\theta_H}$ is completely removed from the Lagrangian. However, the trick does not work for θ_1 and θ_α because (i) χ_1 and N_1 have Majorana mass terms, i.e., the absorbed phase will show up in the mass terms[9], unlike χ_2 and $\tilde{\chi}_2$ which have a Dirac mass term, and (ii) removing θ_α by L_α redefinition will make Yukawa couplings, $y_{\alpha i}$, contain θ_α. As we shall see below, radiative corrections to leptogenesis from the dark sector always involve the product of λ_α and λ_{N_1}. To simplify the analysis, we make λ_α real and then the phase of λ_{N_1} will be the only source of the imaginary part.

The lepton asymmetry on flavor α characterized by $\epsilon_{\alpha\alpha}$ is:

$$\epsilon_{\alpha\alpha} = \frac{\Gamma(N_1 \to \ell_\alpha^- H^+) - \Gamma(N_1 \to \ell_\alpha^+ H^-)}{\Gamma(N_1 \to \ell_\alpha^- H^+) + \Gamma(N_1 \to \ell_\alpha^+ H^-) + \Gamma(N_1 \to \chi_1 S)}, \tag{5.2}$$

where we have neglected the loop contribution in the denominator which is subdominant to the tree-level. We also consider the dilution from $N_1 \to \chi_1 S$, which will not generate a lepton asymmetry. Results of $\epsilon_{\alpha\alpha}$'s from different contributions are shown in Appendix C. We would like to make two comments about the structure of the loops in Fig. 6.

- One of the DM loops does not have a mass insertion to flip the chirality of χ_1. In other words, for the bottom-right diagram, lepton number violation required for leptogenesis actually comes from the external N_1 unlike the other loop diagrams in Fig. 6. In the limit of $m_{N_1} >> m_{\chi_1}$, it would be the dominant contribution.

- As mentioned before, particles in the loop have to be on-shell. Consequently, the sum of m_{χ_1} and m_S has to be smaller than m_{N_1} as seen easily from terms like $B_0(m_{N_1}^2, m_S^2, m_{\chi_1}^2)$ in $\epsilon_{\alpha\alpha}$, where B_0 is the Passarino-Veltman Integral [74].

In terms of $\epsilon_{\alpha\alpha}$, the generated lepton asymmetry $Y_{\Delta L}$ through N_1 decays and the resulting baryon asymmetry $Y_{\Delta B}$ can be expressed as [75]

$$Y_{\Delta B} = C Y_{\Delta L} = C \frac{135\zeta(3)}{4\pi^4 g_*} \sum_\alpha \epsilon_{\alpha\alpha} \eta_\alpha, \tag{5.3}$$

[9]The real scalar S has the same property as well.

where g_* is the relativistic degrees of freedom when N_1 decays.[10] η_α characterizes the washout effect,[11] and C ($= -28/79$) [76, 77] comes from the conversion of ΔL into ΔB by the sphaleron [78–80]. For recent reviews on leptogenesis, see, for example, Refs. [75, 81, 82].

6 DM, θ_{13} and Leptogenesis

Combining all ingredients discussed above, one can check if the DM loop with λ_e and $\lambda_{c(=1)}$ only can alter U_{TBM} into U_{PMNS}, and concurrently accommodate leptogenesis and DM. The difficulty, however, arises from leptogenesis consideration. If only the DM loop contribution is considered, the zero tree-level $N_1 \to L_e^{\mp} H^{\pm}$ (from $(U_{TBM})_{13} = 0$) yields a vanishing lepton asymmetry, recalling that the lepton asymmetry requires both the tree- and loop-level contribution. On top of that, the original leptogenesis (top panels of Fig. 6) does not work either on account of small Yukawa couplings unless the resonance enhancement is involved as we shall see below. To circumvent the problem, one could in principle involve more parameters in the game. With the spirit of minimality in mind, we have two simplest options as follows.

1. With the additional λ_μ, one might expect that $(\delta m_D)_{13}$, from λ_e (and λ_{N_1}), can lead to sizable θ_{13}, while $(\delta m_D)_{23}$, from λ_μ (and λ_{N_1}), is responsible for leptogenesis. From Eq. 5.3 and those in Appendix C, one can infer, in the limit of $m_{N_1} \gg m_\chi,\, m_S$,

$$\left(\frac{Y_{\Delta B}}{10^{-10}}\right) \sim \left(\frac{m_{\chi_1}}{m_{N_1}}\right) \left(\frac{\lambda_{H\chi} \mathrm{Im}\,(\lambda_{N_1})\, \lambda_e}{10^{-10}}\right) \left(\frac{10^{-6}}{y_{\alpha i}}\right). \tag{6.1}$$

   With $\lambda_{H\chi} \sim 0.1$ from the relic density consideration, successful leptogenesis requires $|\lambda_e \mathrm{Im}\,(\lambda_{N_1})\,| \sim 10^{-9}$ for TeV N's and sub-TeV m_χ and m_S. On the other hand, for the NH case, generating sizable θ_{13} demands[12]

$$(\delta m_D)_{13} \sim \frac{1}{16\pi^2} (\lambda_{H\chi} \lambda_{N_1} \lambda_\mu) \frac{v}{\sqrt{2}} \sim \sqrt{2 m_{N_1} m_{\nu_3}} \sin\theta_{13}. \tag{6.2}$$

   It implies $|\lambda_\mu \lambda_{N_1}| \sim 10^{-4}$. In order not to dilute the lepton asymmetry from N_1 decaying into S and χ_1 , λ_{N_1} has to be much smaller than Yukawa couplings ($\sim 10^{-6}$). This implies $\lambda_\mu \gtrsim 10$, and perturbativity is lost.

2. One can also include λ_{N_2} to the model besides λ_e and λ_{N_1}. λ_{N_1} and λ_e are used to accomplish leptogenesis while λ_{N_2} and λ_e give rise to required perturbation on U_{TBM}.[13]

[10] In our case, it is 106.75 (from the SM particles)+ 1 (from S) + $\frac{7}{8} \times 2$ (from χ_1)+ $\frac{7}{8} \times 4$ (from χ_2 and $\tilde{\chi}_2$).

[11] We follow methods used in Ref. [75] to estimate η_α.

[12] It can be derived by simply equating Eq. 3.7 with $\left(U^*_{PMNS} \cdot \mathrm{diag}(m_{\nu_1}, m_{\nu_2}, m_{\nu_3}).U^\dagger_{PMNS}\right)$, and taking the limit of $m_{\nu_{1,2}} \ll m_{\nu_3}$. The same approach can be applied to the IH case, with $m_{\nu_1} \sim m_{\nu_2} \sim m_{\nu_3}$ for $m_{\nu_3} = 0.1$ eV.

[13] Alternatively, θ_{13} can arise from N_1 (λ_{N_1}) while leptogenesis comes from N_2 (λ_{N_2}). Although the generated lepton asymmetry from N_2 will in principle be washed out by N_1 decays, there exist situations [83–88] where the asymmetry survives from N_1 washout effects.

This option, however, suffers from new washout effects from $\chi_1 + S \leftrightarrow H^{\pm} + L^{\mp}$ since Majorana χ_1 can not carry the lepton number. For $m_{N_1} \lesssim 10^7$ GeV [89, 90], washout effects are generally faster than the expansion of the universe, erasing the lepton asymmetry from N_1 decays.

Alternatively, one can employ the resonant enhancement to achieve low-scale leptogenesis [91, 92], i.e., $m_{N_2} - m_{N_1} \sim \Gamma_{N_2}$ (N_2 decay width). We here adopt this method to perform χ^2 fits. To sum up, with a single DM loop associated with $(\delta m_D)_{13}$, the R matrix becomes complex and low-scale leptogenesis can be realized via the resonant enhancement such that the sufficient lepton asymmetry survives from the washout effects. In this situation, the only CP-violation source comes from the phase of λ_{N_1}, inducing a connection between δ_{CP} in U_{PMNS} and leptogenesis.

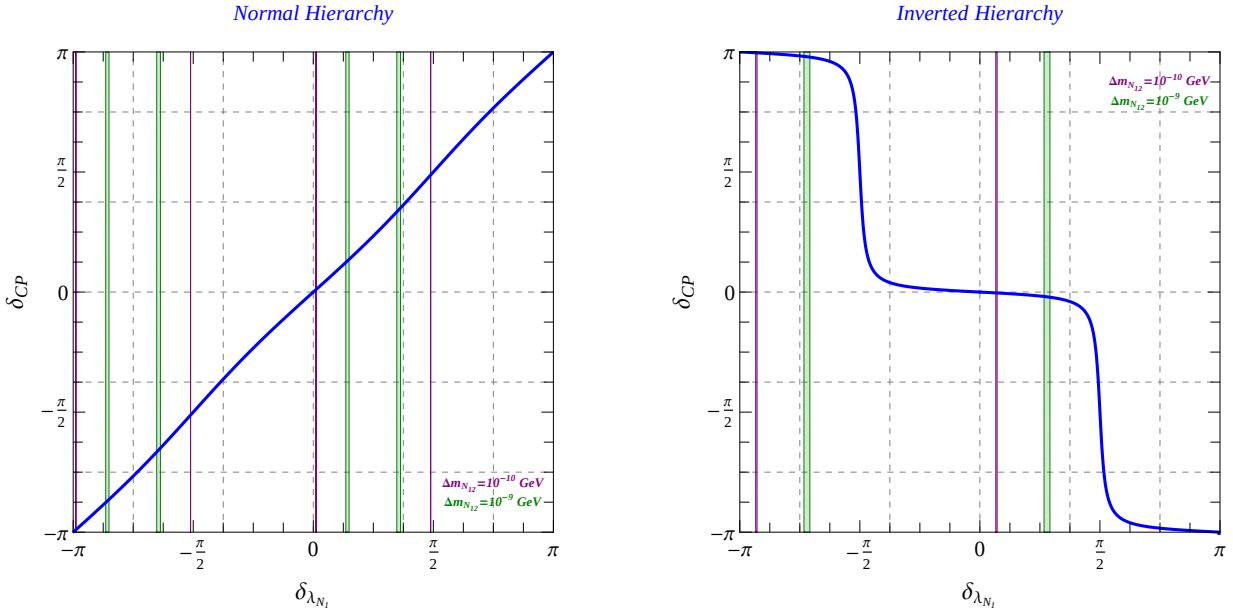

Figure 7: *In the case of TeV N_1, confidence region in green (purple) on the phase of λ_{N_1}, $\delta\lambda_{N_1}$, for $m_{N_2} - m_{N_1} \equiv \Delta m_{N_{12}} = 10^{-9}$ (10^{-10}) GeV. The blue line represents the correlation between $\delta\lambda_{N_1}$ and δ_{CP} in U_{PMNS}.*

The fitting procedure is as follows. The set of parameters involved are presented in Table 3 with $(N_a, N_b, N_c) = (N_3, N_2, N_1)$ and $\Delta m_{N_{12}} = 10^{-9}$ and 10^{-10} GeV. Second, we vary λ_{N_1} to find minimum χ^2 taking into account all observables in Table 2. Then, we fix $|\lambda_{N_1}|$ to the best-fit value and vary its phase $\delta_{\lambda_{N_1}}$. The results are shown in Fig. 7, where the green (purple) band corresponds to the 99% confidence region on $\delta_{\lambda_{N_1}}$ for $\Delta m_{N_{12}} = 10^{-9}$ (10^{-10}) GeV. We also display the corresponding δ_{CP}, ranging from $-\pi$ to π as a function of $\delta_{\lambda_{N_1}}$, with the blue line.[14] We have few observations based on Fig. 7.

[14] Again, θ_{12}, θ_{23} and θ_{13} are constrained to the first quadrant and Majorana phases range from 0 to π as discussed in Refs. [64, 65].

- For the NH case, δ_{CP} is almost linearly proportional to $\delta_{\lambda_{N_1}}$, which is not the case for the IH case. It is due to different chosen values for m_{ν_1} and m_{ν_3}. In other words, if m_{ν_3} is zero, the linear proportionality will show up.

- The lepton symmetry is actually proportional to the imaginary part of $\exp(2i\delta_{\lambda_{N_1}})$ due to the fact $Y_{\Delta L_\mu}$ and $Y_{\Delta L_\tau}$ cancel each other because of the TBM pattern. Therefore, there will be no lepton asymmetry generated if $\delta_{\lambda_{N_1}} = \pm\pi/2$. Furthermore, the physical range of $\delta\lambda_{N_1}$ can be divided into four quadrants; two of them generate positive ΔY_L while the other two produce needed negative ΔY_L for the positive baryon asymmetry.

- The position of the confidence region depends on the maximal ΔY_L at $\delta\lambda_{N_1} = (\pi/4, -3\pi/4)$. If the maximal value is much larger than the required $|\Delta Y_L|$ ($\sim 10^{-10}$), then the confidence region will be located near 0, $\pm\pi/2$ and $-\pi$ as in the NH case with $\Delta m_{N_{12}} = 10^{-10}$ GeV. For the IH case with $\Delta m_{N_{12}} = 10^{-9}$ GeV, the corresponding maximal value is quite close to 10^{-10}, shifting the confidence to be around $\pi/4$ and $-3\pi/4$.

- With $\Delta m_{N_{12}}$ closer to Γ_{N_2} ($\sim 10^{-11}$ GeV), the resonant enhancement becomes larger. That is why the confidence regions (purple ones) with $\Delta m_{N_{12}} = 10^{-10}$ GeV move toward to 0, $\pm\pi/2$ and $-\pi$ with respect to those of $\Delta m_{N_{12}} = 10^{-9}$ GeV. For the IH case, $\delta_{\lambda_{N_1}} \sim \pm\pi/2$ can not reproduce the correct U_{PMNS} mixing angles and the mass-squared differences.

- It is quite interesting that the NH case has a confidence region near $\delta_{CP} = -\pi/2$, which is preferred by the combined T2K and reactor measurements [27].

To conclude, for TeV N_1, the simplest setup to reproduce observables in Table 2 in the presence of the flavor symmetry is to involve only $(\delta m_D)_{13}$, leading to the complex R matrix such that low-mass leptogenesis can be achieved by the resonant enhancement, $m_{N_2} - m_{N_1} \sim \Gamma_{N_2}$.

7 S as inflaton

In this section, we repeat the fitting procedure with m_S and m_{N_i} of 10^{13} GeV, a very different mass scale from the previous sections, in the context of the scalar S being the inflaton ϕ. Recently, the BICEP2 experiment has reported a signal of inflationary gravitational waves in the B-mode power spectrum [36], which could be a hint of inflation. We here explore the possibility of the scalar S being the inflaton with the quadratic chaotic inflation [93]. We start with the summary of relevant equations on inflation. For recent reviews on inflation, see, for instance, Refs. [94–96]. In the limit of slow-roll inflation, the density (scalar) and

tensor perturbations are related to the inflation potential $V(\phi)$ as:

$$\begin{aligned}\Delta_s^2 &\approx \frac{1}{24\pi^2}\frac{V(\phi)}{M_{\rm pl}^4}\frac{1}{\epsilon_V},\\ \Delta_t^2 &\approx \frac{2}{3\pi^2}\frac{V(\phi)}{M_{\rm pl}^4},\end{aligned} \tag{7.1}$$

where $M_{\rm pl}$ is the reduced Planck mass $(8\pi G)^{-1/2}$ $(= 2.4\times 10^{18}$ GeV) and

$$\epsilon_V = \frac{M_{\rm pl}^2}{2}\left(\frac{V'}{V}\right)^2\Bigg|_{\phi=\phi_{\rm cmb}} = 2\left(\frac{M_{\rm pl}}{\phi_{\rm cmb}}\right)^2, \tag{7.2}$$

in which $V' = dV/d\phi$ and $\phi_{\rm cmb}$ is the initial value of the inflaton field required to produce the observed Cosmic Microwave Background (CMB) fluctuations. $\phi_{\rm cmb}$ is related to e-folds $N_{\rm cmb}$ by

$$\phi_{\rm cmb} = 2\sqrt{N_{\rm cmb}}M_{\rm pl}, \tag{7.3}$$

with $N_{\rm cmb}\sim 40-60$. It implies ϕ_{cmb} will be super-Planckian and any flavor models based on effective theory approach will break down. Therefore, when construction concrete UV-complete flavor models, one has to find a way to highly suppress higher order terms like ϕ^4 so that $m^2\phi^2$ is dominant even with super-Planckian values for the inflaton. Consequently, we have

$$\epsilon_V = \frac{1}{2N_{\rm cmb}}. \tag{7.4}$$

From the *Planck* results [97], the scalar perturbation amplitude for $V = m_\phi^2\phi^2$ is 2.2×10^{-9}, [15] which in turns implies $m_\phi\sim 10^{13}$ GeV. Furthermore, the tensor-to-scalar ratio r is,

$$r = \frac{\Delta_t^2}{\Delta_s^2}\approx 16\epsilon_V = \frac{8}{N_{\rm cmb}}\sim 0.16, \tag{7.5}$$

which is consistent with the BICEP2 results with $r = 0.20^{+0.07}_{-0.05}$ or $r = 0.16^{+0.06}_{-0.05}$ after subtracting various dust models [36]. In addition, the scalar spectral index, evaluated at CMB scales,

$$n_s = 1 - \frac{2}{N_{\rm cmb}}\sim 0.96, \tag{7.6}$$

which is also consistent with the *Planck* results [97].

In the situation of S being the inflaton with $m_S\sim 10^{13}$ GeV, to achieve leptogenesis and sizable θ_{13}, one has to make $m_{N_i}\gtrsim m_S$. In this case, unlike the previous situation with TeV N_1, leptogenesis can be realized without resorting to the resonant enhancement since the heavy neutrinos satisfy the mass bounds, $m_{N_1} > 10^9$ GeV [73] and $m_{N_1} > 10^7$ GeV [89]. We have found that one needs only $(\delta m_D)_{13}$ to reproduce the neutrino mixing angles and generate the correct lepton asymmetry.

[15] In fact, many inflation models have similar values of the scalar perturbation amplitude.

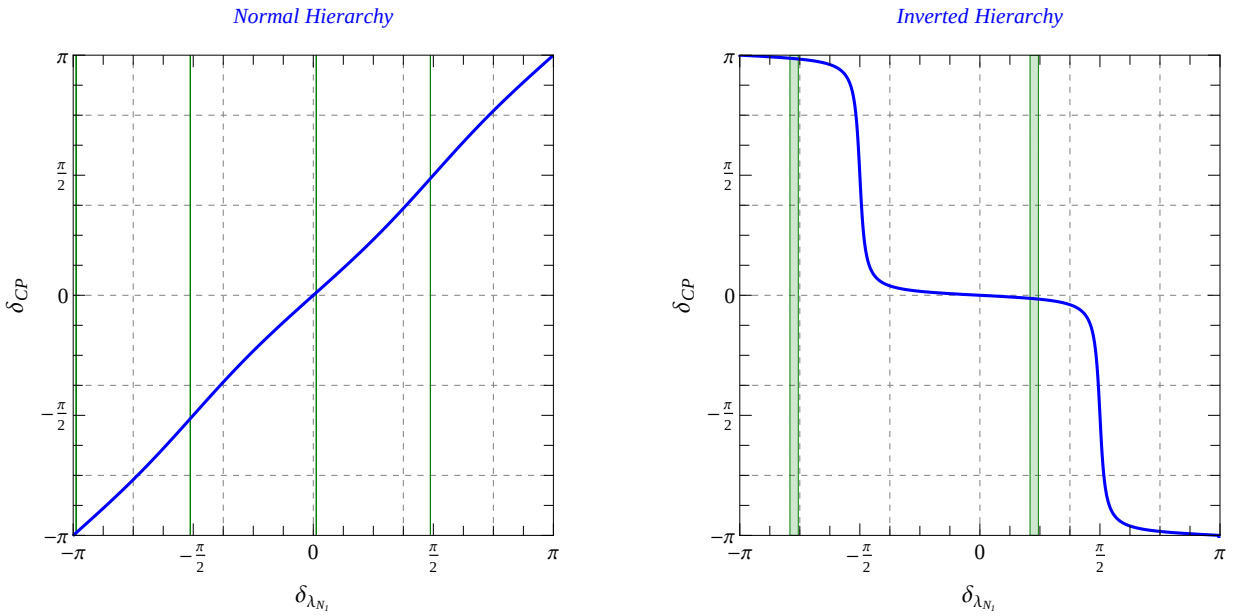

Figure 8: *Confidence region in green on $\delta\lambda_{N_1}$ in the case of S as the inflaton. The blue line represents the correlation between $\delta\lambda_{N_1}$ and δ_{CP}.*

	m_{ν_1} (eV)	m_{ν_2} (eV)	m_{ν_3} (eV)	λ_{N_a}	λ_{N_b}	λ_μ	λ_τ
NH	0	8.66×10^{-3}	4.89×10^{-2}	0	0	0	0
IH	1.107×10^{-1}	1.11×10^{-1}	0.1	0	0	0	0
	m_{N_1} (GeV)	m_{N_2} (GeV)	m_{N_3} (GeV)	m_S (GeV)	m_{χ_1} (GeV)	m_{χ_2} (GeV)	λ_e
NH/IH	1.65×10^{13}	3×10^{13}	4.5×10^{13}	1.5×10^{13}	62	200	1

Table 4: *The Benchmark point for m_N's and m_S around the inflation scale, 10^{13} GeV.*

We adopt the same fitting produce as in Section 6. The results are shown in Fig. 8, where the green band corresponds to the 99% confidence region on $\delta_{\lambda_{N_1}}$, and the blue line represents the correlation between δ_{CP}. We briefly comment on the results, that are quite similar to those of TeV N_1.

- The behavior of the correlation between δ_{CP} and $\delta\lambda_{N_1}$ is the same as in the case of TeV N_1, i.e., determined by the value of m_{ν_1} (m_{n_3}) for NH (IH). Besides, the lepton symmetry is proportional to the imaginary part of $\exp(2i\delta_{\lambda_{N_1}})$ because of the cancellation between $Y_{\Delta L_\mu}$ and $Y_{\Delta L_\tau}$ from the TBM pattern.

- The lepton asymmetry comes from both the original vertex and wave function contribution (top panels of Fig. 6); therefore, m_{N_1} needs not to be close to m_{N_2} as before.

- Washout effects are not very efficient due to the fast expansion of the universe at such a high temperature so that the washout interactions can easily fall out of equilibrium. In addition, due to $m_{\chi_1} \ll m_{N_1}$, χ_1 can carry the same lepton number as L to a very good

approximation. Hence, we do not worry about the aforementioned washout interaction, $\chi_1 + S \leftrightarrow H^{\pm} + L^{\mp}$.

- The NH case also has a confidence region near $\delta_{CP} = -\pi/2$ as above, favored by the combined T2K and reactor measurements [27].

To conclude, for m_S being the inflaton with mass of 10^{13} GeV, the single radiative correction $(\delta m_D)_{13}$ to the Dirac mass matrix m_D can render $\theta_{13} \sim 9^\circ$ and achieve leptogenesis. At the same time, one can have the correct DM density. It also ties the CP-violating phase δ_{CP} in U_{PMNS} with leptogenesis, that is absent from the original type-I seesaw.

8 Conclusions

In the type-I seesaw, θ_{13} is zero if there exists an underlying residual $\mu-\tau$ symmetry. Furthermore, leptogenesis, requiring the complex R matrix [33] characterizing heavy-light neutrino mixing, can not be achieved since a discrete flavor symmetry renders R matrix real and diagonal. Assuming the underlying residual flavor symmetry predicts the TBM neutrino mixing pattern, we here propose a simple toy model, where the additional particles, including the DM candidate, are introduced to break the residual flavor symmetry. Explicitly, an $SU(2)_L$ singlet fermion χ_1, which is the DM candidate, a fermonic $SU(2)_L$ doublet χ_2 and a real gauge-singlet scalar S generate the radiative corrections, δm_D, to the neutrino Dirac mass matrix, leading to $\theta_{13} \sim 9^\circ$ and providing both CP-violating and CP-conserving phases for leptogenesis. These additional particles are odd under the imposed Z_2 symmetry, which is used to guarantee the DM stability.

Keeping a spirit of minimality, we look for the minimum setup to achieve the aforementioned goals. We have found, for TeV right-handed neutrinos and sub-TeV χ's and S, one needs resonant leptogenesis, i.e., the mass difference between N_1 and N_2 is close to the decay width of N_2. Otherwise, strong washout interactions lead to an insufficient lepton asymmetry. In this case, one requires only $(\delta m_D)_{13}$ to simultaneously accommodate sizable θ_{13} and leptogenesis, leading a connection between the CP phase in the neutrino mixing matrix and leptogenesis. Interesting, with a small $N_1 - N_2$ mass splitting in the NH case, the complex phase from the DM loop can generate $\delta_{CP} \simeq -\pi/2$ favored by the T2K experiment [27].

On the other hand, in light of the recent BICEP2 results of the scalar-to-tensor ratio [36], S being the inflaton, with the quadratic potential and the mass of 10^{13} GeV, can explain the BICEP2 results very well. In this case, with the heavy neutrino mass of the same order, one also requires only $(\delta m_D)_{13}$ to simultaneously accommodate sizable θ_{13} and leptogenesis, because the corresponding Yukawa couplings are large enough to generate the lepton symmetry without the DM loop contribution or the resonance enhancement. Similarly, one of the confidence regions on $\delta_{\lambda_{N_1}}$ in NH corresponds to $\delta_{CP} \simeq -\pi/2$ preferred by the experiment.

Finally, we would like to point out radiative corrections coming from particles outside of the dark sector could also render θ_{13} nonzero. It would, of course, spoil the connection between

DM and neutrino physics advertised here. Therefore, one has to find a way to suppress or forbid these kinds of corrections when building concrete models.

Acknowledgments

The author is especially thankful to Frank Deppisch, Valerie Domcke, Alfredo Urbano and Diego Aristizabal Sierra for many precious and enlightening discussions. The author thanks Frank Deppisch, Jennifer Kile, Valerie Domcke and Alfredo Urbano for very useful comments on the draft, and John Ellis for pointing out the correlation between δ_{CP} and leptogenesis. The author thanks Chee Sheng Fong for indicating important washout effects and very helpful discussions. The author is grateful for the hospitality of Academia Sinica (Taiwan), where this work was initiated. This work is supported by the London Centre for Terauniverse Studies (LCTS), using funding from the European Research Council via the Advanced Investigator Grant 267352.

A Toy Model in A_4

In this Section, we construct a simple toy model in A_4, which mimics the model from Ref. [98] to demonstrate how the dark sector violates the residual flavor symmetry, which leads to the TBM pattern.

The Lagrangian reads,

$$\mathcal{L} \supset \mathcal{L}_1 + \mathcal{L}_2, \tag{A.1}$$

with

$$\begin{aligned} \mathcal{L}_1 &= yLHN + \frac{\phi_E}{\Lambda} L\tilde{H}\left(y_e e^c + y_\mu \mu^c + y_\tau \tau^c\right) + m_N NN + \kappa \phi_N NN \\ \mathcal{L}_2 &= \lambda L D_2 S + \lambda_{H\chi} D_2 \tilde{H} D_1 + \lambda_N D_1 N S, \end{aligned} \tag{A.2}$$

where $L = (L_e, L_\mu, L_\tau)$, $N = (N_1, N_2, N_3)$, $\phi_{N,E} = (\phi_{N_1,E_1}, \phi_{N_2,E_2}, \phi_{N_3,E_3})$, $D_1 = (\chi_1, sp_1, sp_2)$ and D_2 $(\tilde{D}_2) = (\chi_2\ (\tilde{\chi}_2), sp_3, sp_4)$ are triplets under A_4. Note that we promote χs to A_4 triplets with the help of spurions (sp). On the other hand, one can also involve very massive physical fields into D_i by playing with mass terms of D_i such that the lightest mass eigenstate is χ_i and other massive particles have negligible contributions to the neutrino mass matrix. In any case, A_4 is broken by χs. The particle content and corresponding quantum numbers are shown in Table. 5.

From $\mathcal{L}_1$, with $\langle \phi_E \rangle \sim (v_E, 0, 0)$, the charged lepton mass matrix is diagonal with masses proportional to y_e, y_μ and y_τ, respectively. The neutrino Dirac mass matrix are diagonal, $m_D = y\langle H \rangle \mathbb{1}_{3\times 3}$ while the mass matrix for heavy neutrinos N becomes,

$$M_N = \begin{pmatrix} \frac{2}{3}\kappa\langle\phi_{N_1}\rangle + m_N & -\frac{1}{3}\kappa\langle\phi_{N_2}\rangle & -\frac{1}{3}\kappa\langle\phi_{N_3}\rangle \\ -\frac{1}{3}\kappa\langle\phi_{N_2}\rangle & \frac{2}{3}\kappa\langle\phi_{N_3}\rangle + m_N & -\frac{1}{3}\kappa\langle\phi_{N_1}\rangle \\ -\frac{1}{3}\kappa\langle\phi_{N_3}\rangle & -\frac{1}{3}\kappa\langle\phi_{N_1}\rangle & \frac{2}{3}\kappa\langle\phi_{N_2}\rangle + m_N \end{pmatrix}. \tag{A.3}$$

Field	L	e^c	μ^c	τ^c	H	N	D_1	D_2	$\tilde{D}_2$	S	ϕ_N	ϕ_E
A_4	3	1	$1'$	$1''$	1	3	3	3	3	1	3	3
$SU(2)_L$	2	1	1	1	2	1	1	2	2	1	1	1
$U(1)_Y$	-1/2	1	1	1	1/2	0	0	1/2	-1/2	0	0	0
Z_2	+	+	+	+	+	+	–	–	–	–	+	+

Table 5: *The particle content and corresponding quantum numbers in the toy model based on A_4.*

The resulting light neutrino mass matrix is

$$m_\nu = m_D M_N^{-1} m_D^T, \tag{A.4}$$

and it is easy to verify m_ν can be diagonalized by U_{TBM} if $\langle\phi_{N_1}\rangle = \langle\phi_{N_2}\rangle = \langle\phi_{N_3}\rangle$, i.e.,

$$\hat{m}_\nu = U_{TBM}^T m_\nu U_{TBM}, \tag{A.5}$$

where

$$U_{TBM} = \begin{pmatrix} \sqrt{\frac{2}{3}} & \frac{1}{\sqrt{3}} & 0 \\ -\frac{1}{\sqrt{6}} & \frac{1}{\sqrt{3}} & \frac{1}{\sqrt{2}} \\ -\frac{1}{\sqrt{6}} & \frac{1}{\sqrt{3}} & -\frac{1}{\sqrt{2}} \end{pmatrix}. \tag{A.6}$$

Finally, radiative corrections coming from D_i and S to U_{TBM} will depend on how to embed χ_i into D_i. Clearly, in the presence of spurions or heavy physical fields, the A_4 symmetry is violated. We would like to emphasize again that in this paper, we choose a model independent approach to study the radiative corrections in a spirit of minimality to realize the nonzero θ_{13}, which could serve as a guiding principles to build realistic models.

B DM relic density and DD

In the limit of small $\chi_1 - \chi_2$ mixing angle θ, and $\lambda_{H\chi} = \lambda_{H\tilde{\chi}}$, the annihilation cross section for s-channel Higgs exchange is,

$$\begin{aligned} \langle\sigma v_{rel}\rangle = \quad & \sin^2\theta \left(\sum_f \Theta(m_{\chi_1} - m_f) \frac{\lambda_{H\chi}^2 N_c m_f^2 m_{\chi_1}^2 v_{rel}^2}{4\pi v^2} \frac{(1-r_f)^{3/2}}{\left(4m_{\chi_1}^2 - m_h^2\right)^2 + m_h^2\Gamma_h^2} \right. \\ & + \Theta(m_{\chi_1} - m_W) \frac{\lambda_{H\chi}^2 m_{\chi_1}^4 v_{rel}^2}{8\pi v^2} \frac{(1-r_W^2)^{1/2}(4 - 4r_W + 3r_W^2)}{\left(4m_{\chi_1}^2 - m_h^2\right)^2 + m_h^2\Gamma_h^2} \\ & \left. + \Theta(m_{\chi_1} - m_Z) \frac{\lambda_{H\chi}^2 m_{\chi_1}^4 v_{rel}^2}{16\pi v^2} \frac{(1-r_Z^2)^{1/2}(4 - 4r_Z + 3r_Z^2)}{\left(4m_{\chi_1}^2 - m_h^2\right)^2 + m_h^2\Gamma_h^2} \right), \end{aligned} \tag{B.1}$$

where $r_i = (m_i/m_{\chi_1})^2$ for $i = (f, W, Z)$, v_{rel} is the relative velocity, and N_c is the color factor: 3 (1) for quarks (leptons). m_f, m_W and m_Z are the masses for final state fermions, W and Z boson, respectively. The step function Θ manifests the kinematical constraint. With $\langle\sigma v_{rel}\rangle$, one can compute DM abundance including the thermal effect that is very important for the resonant enhancement. We refer readers to Ref. [99] for more details.

The SI DM-nucleon cross-section via Higgs exchange is [100],

$$\sigma_{SI} = c_{DM} \sin^2\theta \frac{\mu_\chi^2}{\pi} \frac{(\lambda_{H\chi} M_N f_N)^2}{2 m_h^4 v^2}, \tag{B.2}$$

where $c_{DM} = 1$ ($c_{DM} = 4$) for Dirac (Majorana) DM, M_N is the nucleon mass, μ_χ is the reduced DM-nucleon mass $\frac{m_{\chi_1} M_N}{m_{\chi_1} + M_N}$, $f_N = 0.34$ [101], and v is the Higgs VEV(~ 246) GeV.

C $\epsilon_{\alpha\alpha}$ in Leptogenesis computation

Here we present $\epsilon_{\alpha\alpha}$'s for three different situations: the original type-I seesaw leptogenesis, the degenerate case ($m_{N_2} - m_{N_1} \sim \Gamma_{N_2}$), the DM loop contributions, respectively.

From Ref. [102], $\epsilon_{\alpha\alpha}$ in the original type-I seesaw leptogenesis, consisting of the vertex and wave function contribution, is

$$\begin{aligned}\epsilon_{\alpha\alpha} = \quad & \frac{1}{8\pi} \sum_{j\neq 1} \sum_{\beta} f(r_j) \frac{\mathrm{Im}\left[y^*_{\alpha j} y_{\alpha 1} y^*_{\beta j} y_{\beta 1}\right]}{(y^\dagger y)_{11} + |\lambda_{N_1}|^2 g_{kin}} \\ & - \frac{1}{8\pi} \sum_{j\neq 1} \frac{m_{N_1}}{m^2_{N_j} - m^2_{N_1}} \frac{\mathrm{Im}\left\{\left[m_{N_j} \left(y^\dagger y\right)_{j1} + m_{N_1} \left(y^\dagger y\right)_{1j}\right] y^*_{\alpha j} y_{\alpha 1}\right\}}{(y^\dagger y)_{11} + |\lambda_{N_1}|^2 g_{kin}},\end{aligned} \tag{C.1}$$

where $r_j \equiv m^2_{N_j}/m^2_{N_1}$, $f(x) = \sqrt{x}(1 - (1+x)\ln[(1+x)/x])$ and

$$g_{kin} = \frac{2\left(m^2_{N_1} - m^2_S + m^2_{\chi_1}\right)}{m^3_{N_1}} \sqrt{\frac{\left(m^2_{N_1} - m^2_S + m^2_{\chi_1}\right)^2}{4 m^2_{N_1}} - m^2_{\chi_1}}. \tag{C.2}$$

We here include the dilution from $N_1 \to \chi_1 S$, which does not generate the lepton asymmetry.

In the limit of N_1 and N_2 being degenerate ($m_{N_2} - m_{N_1} \sim \Gamma_{N_2}$), where the lepton asymmetry is dominated by the wave function contribution, we have [91, 92][16]

$$\epsilon_{res} = \frac{\mathrm{Im}\left[\left(y^\dagger y\right)_{12}\right]^2}{\left((y^\dagger y)_{11} + |\lambda_{N_1}|^2 g_{kin}\right)(y^\dagger y)_{22}} \frac{\left(m^2_{N_2} - m^2_{N_1}\right) m_{N_1} \Gamma_{N_2}}{\left(m^2_{N_2} - m^2_{N_1}\right)^2 + m^2_{N_1} \Gamma^2_{N_2}}, \tag{C.3}$$

where we have summed over all lepton flavors.

[16] Note that we have a different definition of Yukawa couplings from the Refs.

For the lepton asymmetry generated from the DM loop, $\epsilon_{\alpha\alpha}$ can be written as,

$$\epsilon_{\alpha\alpha} = 2\frac{\mathrm{Im}\left(y^*_{\alpha 1}\lambda^*_1\lambda_{H\chi}\lambda_\alpha\right)\mathrm{Im}\left(f_{A_1}\right) + \mathrm{Im}\left(y^*_{\alpha 1}\lambda_{N_1}\lambda_{H\chi}\lambda_\alpha\right)\mathrm{Im}\left(f_{A_2}\right)}{(y^\dagger y)_{11} + |\lambda_{N_1}|^2 g_{kin}}, \tag{C.4}$$

where

$$\begin{aligned} f_{A_1} = \quad & \frac{m_{N_1} m_{\chi_1}}{16\pi^2\left(m^2_{N_1} - m^2_h\right)}\left(\left(m^2_S - m^2_{\chi_2}\right)C_0(m^2_h, 0, m^2_{N_1}, m^2_{\chi_1}, m^2_{\chi_2}, m^2_S)\right. \\ & \left. + B_0(m^2_h, m^2_{\chi_1}, m^2_{\chi_2}) - B_0(m^2_{N_1}, m^2_S, m^2_{\chi_1})\right), \end{aligned} \tag{C.5}$$

and

$$\begin{aligned} f_{A_2} = \quad & \frac{1}{16\pi^2\left(m^2_{N_1} - m^2_h\right)}\left(\left(m^2_S m^2_h - m^2_{N_1} m^2_{\chi_2}\right)C_0(m^2_h, 0, m^2_{N_1}, m^2_{\chi_1}, m^2_{\chi_2}, m^2_S)\right. \\ & \left. + m^2_h B_0(m^2_h, m^2_{\chi_1}, m^2_{\chi_2}) - m^2_{N_1} B_0(m^2_{N_1}, m^2_S, m^2_{\chi_1})\right). \end{aligned} \tag{C.6}$$

B_0 and C_0 are Passarino-Veltman Integrals [74]. Note that if N_1 decays before the electroweak phase transition, then the Higgs boson is massless, i.e., $m_h = 0$.

References

[1] P. Minkowiski, Phys. Lett. B **67**, 421 (1977); M. Gell-Mann, P. Ramond and R. Slansky in *Supergravity*, eds. D. Freedman and P. Van Niuenhuizen (North Holland, Amsterdam, 1979), p. 315; T. Yanagida in *Proceedings of the Workshop on Unified Theory and Baryon Number in the Universe*, eds. O. Sawada and A. Sugamoto (KEK, Tsukuba, Japan, 1979); S.L. Glashow, *1979 Cargèse Lectures in Physics — Quarks and Leptons*, eds. M. Lévy *et al.* (Plenum, New York, 1980), p. 707. See also R.N. Mohapatra and G. Senjanović, Phys. Rev. Lett. **44**, 912 (1980) and J. Schechter and J.W.F. Valle, Phys. Rev. D **22**, 2227 (1980). .

[2] P. Harrison, D. Perkins, and W. Scott, Phys.Lett. **B530**, 167 (2002), hep-ph/0202074.

[3] P. Harrison and W. Scott, Phys.Lett. **B535**, 163 (2002), hep-ph/0203209.

[4] Z.-z. Xing, Phys.Lett. **B533**, 85 (2002), hep-ph/0204049.

[5] P. Harrison and W. Scott, Phys.Lett. **B547**, 219 (2002), hep-ph/0210197.

[6] P. Harrison and W. Scott, Phys.Lett. **B557**, 76 (2003), hep-ph/0302025.

[7] P. Harrison and W. Scott, Phys.Lett. **B594**, 324 (2004), hep-ph/0403278.

[8] E. Ma and G. Rajasekaran, Phys.Rev. **D64**, 113012 (2001), hep-ph/0106291.

[9] K. Babu, E. Ma, and J. Valle, Phys.Lett. **B552**, 207 (2003), hep-ph/0206292.

[10] E. Ma, Phys.Rev. **D73**, 057304 (2006), hep-ph/0511133.

[11] G. Altarelli and F. Feruglio, Nucl.Phys. **B741**, 215 (2006), hep-ph/0512103.

[12] S. F. King and M. Malinsky, Phys.Lett. **B645**, 351 (2007), hep-ph/0610250.

[13] Y. Lin, Nucl.Phys. **B813**, 91 (2009), 0804.2867.

[14] M.-C. Chen and S. F. King, JHEP **0906**, 072 (2009), 0903.0125.

[15] C. Hagedorn, M. Lindner, and R. Mohapatra, JHEP **0606**, 042 (2006), hep-ph/0602244.

[16] G. Altarelli, F. Feruglio, and L. Merlo, JHEP **0905**, 020 (2009), 0903.1940.

[17] F. Bazzocchi, L. Merlo, and S. Morisi, Nucl.Phys. **B816**, 204 (2009), 0901.2086.

[18] P. Bhupal Dev, R. Mohapatra, and M. Severson, Phys.Rev. **D84**, 053005 (2011), 1107.2378.

[19] P. Bhupal Dev, B. Dutta, R. Mohapatra, and M. Severson, Phys.Rev. **D86**, 035002 (2012), 1202.4012.

[20] M.-C. Chen and K. Mahanthappa, Phys.Lett. **B652**, 34 (2007), 0705.0714.

[21] M.-C. Chen and K. Mahanthappa, Phys.Lett. **B681**, 444 (2009), 0904.1721.

[22] A. Meroni, S. Petcov, and M. Spinrath, Phys.Rev. **D86**, 113003 (2012), 1205.5241.

[23] DOUBLE-CHOOZ Collaboration, Y. Abe *et al.*, Phys.Rev.Lett. **108**, 131801 (2012), 1112.6353.

[24] DAYA-BAY Collaboration, F. An *et al.*, Phys.Rev.Lett. **108**, 171803 (2012), 1203.1669.

[25] RENO collaboration, J. Ahn *et al.*, Phys.Rev.Lett. **108**, 191802 (2012), 1204.0626.

[26] MINOS Collaboration, P. Adamson *et al.*, Phys.Rev.Lett. **110**, 171801 (2013), 1301.4581.

[27] T2K Collaboration, K. Abe *et al.*, Phys.Rev.Lett. **112**, 061802 (2014), 1311.4750.

[28] D. Aristizabal Sierra, F. Bazzocchi, I. de Medeiros Varzielas, L. Merlo, and S. Morisi, Nucl.Phys. **B827**, 34 (2010), 0908.0907.

[29] E. E. Jenkins and A. V. Manohar, Phys.Lett. **B668**, 210 (2008), 0807.4176.

[30] E. Bertuzzo, P. Di Bari, F. Feruglio, and E. Nardi, JHEP **0911**, 036 (2009), 0908.0161.

[31] C. Hagedorn, E. Molinaro, and S. Petcov, JHEP **0909**, 115 (2009), 0908.0240.

[32] R. G. Felipe and H. Serodio, Phys.Rev. **D81**, 053008 (2010), 0908.2947.

[33] J. Casas and A. Ibarra, Nucl.Phys. **B618**, 171 (2001), hep-ph/0103065.

[34] C. I. Low and R. R. Volkas, Phys.Rev. **D68**, 033007 (2003), hep-ph/0305243.

[35] S. Choubey, S. King, and M. Mitra, Phys.Rev. **D82**, 033002 (2010), 1004.3756.

[36] BICEP2 Collaboration, P. Ade *et al.*, (2014), 1403.3985.

[37] G. D'Ambrosio, G. Giudice, G. Isidori, and A. Strumia, Nucl.Phys. **B645**, 155 (2002), hep-ph/0207036.

[38] J. March-Russell, C. McCabe, and M. McCullough, JHEP **1003**, 108 (2010), 0911.4489.

[39] B. Batell, J. Pradler, and M. Spannowsky, JHEP **1108**, 038 (2011), 1105.1781.

[40] P. Agrawal, S. Blanchet, Z. Chacko, and C. Kilic, Phys.Rev. **D86**, 055002 (2012), 1109.3516.

[41] J. Kile and A. Soni, Phys.Rev. **D84**, 035016 (2011), 1104.5239.

[42] J. F. Kamenik and J. Zupan, Phys.Rev. **D84**, 111502 (2011), 1107.0623.

[43] B. Batell, T. Lin, and L.-T. Wang, JHEP **1401**, 075 (2014), 1309.4462.

[44] A. Kumar and S. Tulin, Phys.Rev. **D87**, 095006 (2013), 1303.0332.

[45] L. Lopez-Honorez and L. Merlo, Phys.Lett. **B722**, 135 (2013), 1303.1087.

[46] J. Kile, (2013), 1308.0584.

[47] T. Hambye, K. Kannike, E. Ma, and M. Raidal, Phys.Rev. **D75**, 095003 (2007), hep-ph/0609228.

[48] M. Hirsch, S. Morisi, E. Peinado, and J. Valle, Phys.Rev. **D82**, 116003 (2010), 1007.0871.

[49] M. Boucenna *et al.*, JHEP **1105**, 037 (2011), 1101.2874.

[50] Y. Ahn and H. Okada, Phys.Rev. **D85**, 073010 (2012), 1201.4436.

[51] E. Ma, A. Natale, and A. Rashed, Int.J.Mod.Phys. **A27**, 1250134 (2012), 1206.1570.

[52] Particle Data Group, J. Beringer *et al.*, Phys.Rev. **D86**, 010001 (2012).

[53] T2K Collaboration, K. Abe *et al.*, Phys.Rev.Lett. **111**, 211803 (2013), 1308.0465.

[54] Planck Collaboration, P. Ade *et al.*, (2013), 1303.5076.

[55] J. A. Acosta, A. Aranda, M. A. Buen-Abad, and A. D. Rojas, Phys.Lett. **B718**, 1413 (2013), 1207.6093.

[56] J. A. Acosta, A. Aranda, and J. Virrueta, (2014), 1402.0754.

[57] J. Kile, M. J. Prez, P. Ramond, and J. Zhang, (2014), 1403.6136.

[58] U. Seljak, A. Slosar, and P. McDonald, JCAP **0610**, 014 (2006), astro-ph/0604335.

[59] S. Joudaki, Phys.Rev. **D87**, 083523 (2013), 1202.0005.

[60] J.-Q. Xia *et al.*, JCAP **1206**, 010 (2012), 1203.5105.

[61] S. Riemer-Sorensen, D. Parkinson, T. M. Davis, and C. Blake, Astrophys.J. **763**, 89 (2013), 1210.2131.

[62] G.-B. Zhao *et al.*, Mon.Not.Roy.Astron.Soc. **436**, 2038 (2013), 1211.3741.

[63] S. Riemer-Srensen, D. Parkinson, and T. M. Davis, (2013), 1306.4153.

[64] A. de Gouvea and J. Jenkins, Phys.Rev. **D78**, 053003 (2008), 0804.3627.

[65] A. de Gouvea, W.-C. Huang, and S. Shalgar, Phys.Rev. **D84**, 035011 (2011), 1007.3664.

[66] E. Ma, Phys.Rev. **D66**, 117301 (2002), hep-ph/0207352.

[67] J. Liao, D. Marfatia, and K. Whisnant, Phys.Rev. **D87**, 013003 (2013), 1205.6860.

[68] M. Hirsch, J. Romao, S. Skadhauge, J. Valle, and A. Villanova del Moral, Phys.Rev. **D69**, 093006 (2004), hep-ph/0312265.

[69] LUX Collaboration, D. Akerib *et al.*, Phys.Rev.Lett. **112**, 091303 (2014), 1310.8214.

[70] A. Djouadi, J. Kalinowski, and M. Spira, Comput.Phys.Commun. **108**, 56 (1998), hep-ph/9704448.

[71] M. Tavakoli, I. Cholis, C. Evoli, and P. Ullio, JCAP **1401**, 017 (2014), 1308.4135.

[72] H. K. Dreiner, H. E. Haber, and S. P. Martin, Phys.Rept. **494**, 1 (2010), 0812.1594.

[73] S. Davidson and A. Ibarra, Phys.Lett. **B535**, 25 (2002), hep-ph/0202239.

[74] G. Passarino and M. Veltman, Nucl.Phys. **B160**, 151 (1979).

[75] S. Davidson, E. Nardi, and Y. Nir, Phys.Rept. **466**, 105 (2008), 0802.2962.

[76] S. Y. Khlebnikov and M. Shaposhnikov, Nucl.Phys. **B308**, 885 (1988).

[77] J. A. Harvey and M. S. Turner, Phys.Rev. **D42**, 3344 (1990).

[78] F. R. Klinkhamer and N. Manton, Phys.Rev. **D30**, 2212 (1984).

[79] P. B. Arnold and L. D. McLerran, Phys.Rev. **D36**, 581 (1987).

[80] P. B. Arnold and L. D. McLerran, Phys.Rev. **D37**, 1020 (1988).

[81] W. Buchmuller, R. Peccei, and T. Yanagida, Ann.Rev.Nucl.Part.Sci. **55**, 311 (2005), hep-ph/0502169.

[82] M.-C. Chen, p. 123 (2007), hep-ph/0703087.

[83] R. Barbieri, P. Creminelli, A. Strumia, and N. Tetradis, Nucl.Phys. **B575**, 61 (2000), hep-ph/9911315.

[84] P. Di Bari, Nucl.Phys. **B727**, 318 (2005), hep-ph/0502082.

[85] O. Vives, Phys.Rev. **D73**, 073006 (2006), hep-ph/0512160.

[86] S. Blanchet and P. Di Bari, JCAP **0606**, 023 (2006), hep-ph/0603107.

[87] A. Strumia, p. 655 (2006), hep-ph/0608347.

[88] G. Engelhard, Y. Grossman, E. Nardi, and Y. Nir, Phys.Rev.Lett. **99**, 081802 (2007), hep-ph/0612187.

[89] D. Aristizabal Sierra, C. S. Fong, E. Nardi, and E. Peinado, JCAP **1402**, 013 (2014), 1309.4770.

[90] J. Racker, JCAP **1403**, 025 (2014), 1308.1840.

[91] A. Pilaftsis, Phys.Rev. **D56**, 5431 (1997), hep-ph/9707235.

[92] A. Pilaftsis and T. E. Underwood, Nucl.Phys. **B692**, 303 (2004), hep-ph/0309342.

[93] A. D. Linde, Phys.Lett. **B129**, 177 (1983).

[94] W. H. Kinney, (2009), 0902.1529.

[95] D. Baumann, (2009), 0907.5424.

[96] J. Martin, C. Ringeval, and V. Vennin, (2013), 1303.3787.

[97] Planck Collaboration, P. Ade *et al.*, (2013), 1303.5082.

[98] M.-C. Chen, J. Huang, J.-M. O'Bryan, A. M. Wijangco, and F. Yu, JHEP **1302**, 021 (2013), 1210.6982.

[99] K. Griest and D. Seckel, Phys.Rev. **D43**, 3191 (1991).

[100] G. Belanger, F. Boudjema, A. Pukhov, and A. Semenov, Comput.Phys.Commun. **180**, 747 (2009), 0803.2360.

[101] J. M. Cline, K. Kainulainen, P. Scott, and C. Weniger, Phys.Rev. **D88**, 055025 (2013), 1306.4710.

[102] L. Covi, E. Roulet, and F. Vissani, Phys.Lett. **B384**, 169 (1996), hep-ph/9605319.